Westinghouse

Westinghouse Electric Company
Nuclear Power Plants
P.O. Box 355
Pittsburgh, Pennsylvania 15230-0355
USA

U.S. Nuclear Regulatory Commission
ATTENTION: Document Control Desk
Washington, D.C. 20555

Direct tel: 412-374-2035
Direct fax: 724-940-8505
e-mail: ziesinrf@westinghouse.com

Your ref: Docket No. 52-006
Our ref: DCP_NRC_003040

September 8, 2010

Subject: AP1000 Response to Request for Additional Information (SRP TR85)

Westinghouse is submitting a response to the NRC request for additional information (RAI) on SRP Section TR85. This RAI response is submitted in support of the AP1000 Design Certification Amendment Application (Docket No. 52-006). The information included in this response is generic and is expected to apply to all COL applications referencing the AP1000 Design Certification and the AP1000 Design Certification Amendment Application.

Enclosure 1 provides the response for the following RAI(s):

RAI-TR85-SEB1-32 R5

Questions or requests for additional information related to the content and preparation of this response should be directed to Westinghouse. Please send copies of such questions or requests to the prospective applicants for combined licenses referencing the AP1000 Design Certification. A representative for each applicant is included on the cc: list of this letter.

Very truly yours,

R. F. Ziesing
Director, U.S. Licensing

/Enclosure

1. Response to Request for Additional Information on SRP Section TR85

D063
NRO

cc:	D. Jaffe	-	U.S. NRC	1E
	E. McKenna	-	U.S. NRC	1E
	B. Gleaves	-	U.S. NRC	1E
	T. Spink	-	TVA	1E
	P. Hastings	-	Duke Energy	1E
	R. Kitchen	-	Progress Energy	1E
	A. Monroe	-	SCANA	1E
	P. Jacobs	-	Florida Power & Light	1E
	C. Pierce	-	Southern Company	1E
	E. Schmiech	-	Westinghouse	1E
	G. Zinke	-	NuStart/Entergy	1E
	R. Grumbir	-	NuStart	1E
	D. Lindgren	-	Westinghouse	1E

ENCLOSURE 1

Response to Request for Additional Information on SRP Section TR85

AP1000 TECHNICAL REPORT REVIEW

Response to Request For Additional Information (RAI)

RAI Response Number: RAI-TR85-SEB1-32
Revision: 5

Question:

As shown by the studies in Section 2.7.1.2.1, when the soil is represented as solid elements rather than Winkler soil springs, higher bearing pressures occur at the edges and lower bearing pressures away from the edges. This is referred to as the effects of the Boussinesq distribution. Although this indicates that the basemat slab away from the walls would have higher bearing pressures using the Winkler soil spring approach (see Figure 2.7-2), the calculation of the maximum bearing pressure would still exist at the building edges if the soil is modeled as solid elements. Therefore, explain why the maximum bearing pressure for the AP1000 design, discussed in Section 2.4.2, should be based on the 2D ANSYS nonlinear dynamic analysis using Winkler soil springs rather than solid soil elements?

Additional Request (Revision 1):

The staff reviewed the RAI response submitted in Westinghouse letter dated March 31, 2008, and notes that the outstanding issues raised by this RAI are considered to be very significant. The RAI response states that the DCD "revision now indicates the line of lift-off, thereby defining the maximum total load applied to the foundation at the time of maximum demand...the dynamic bearing capacity is related to the overall loading on the foundation and to the shear strength mobilized over a failure surface in the foundation soils. The local maximum values close to the edge are not significant to this capacity and will redistribute if local stresses in the soil are excessive. This total load rather than a peak stress below an edge is to be considered by the Combined License applicant in demonstrating stability of the foundation material." Westinghouse is requested to address the following:

1. The above statements are not consistent with the criteria in the DCD because the statements indicate that the total load is used by the Combined License applicant to demonstrate the adequacy of the soil whereas, the DCD requires comparison of the maximum bearing pressure demand to bearing pressure capacity (e.g., DCD Tier 2, Section 2.5.4.2 and DCD Tier 1, Chapter 5.). Explain this inconsistency.

2. As noted in the original RAI, the studies in Section 2.7.1.2.1 demonstrate that when the soil is represented as solid elements, higher bearing pressures occur at the edges than when uniform Winkler type soil springs are used. This is a well known behavior in soil mechanics and is referred to as the Boussinesq effect. Since the current dynamic soil bearing pressure demand criterion of 35 ksf is still based on the 2D ANSYS stick model analysis, Westinghouse is requested to either (1) justify the statement that the localized peak soil pressures will redistribute if local stresses in the soil are excessive and the NI will still be stable or (2) explain what is the technical basis for using a uniform soil spring representation rather than soil brick

finite element or a soil spring distribution which more accurately captures the actual pressure distribution beneath the basemat.

3. The proposed revision to DCD Section 2.5.4.2 - Bearing Capacity, states that the "The maximum demand of 35 ksf occurs under the west edge of the shield building and is primarily due to the response to the east-west component of the earthquake. The east edge of the nuclear island lifts off the soil. The Combined License applicant will verify that the site specific allowable soil bearing capacities for static and dynamic loads at the site will exceed this demand. The evaluation may be limited to response in the east-west direction since the bearing demand is lower in the north-south direction." Explain what is meant by the statement that an "evaluation" may be limited to response in the east-west direction, because no "evaluation" or analysis to be performed by the applicant can be located in the DCD; instead the allowable soil bearing capacity needs to be shown to be greater than the bearing demand under static and dynamic loads.

Additional Request (Revision 2):
(Follow-up RAIs dated 4/27/09)

The RAI response indicates that the seismic analysis for determining the soil bearing pressure demand has been revised to utilize the SASSI 3D finite element NI20 model using a seismic time history soil-structure interaction analysis. This analysis was performed for the hard rock case and five soil conditions. The model includes a surrounding layer of excavated soil and the existing soil media. The soil media in SASSI is an idealization of the various horizontal soil layers. This representation of the soil in SASSI is considered to be more realistic and accurate than the uniform Winkler type soil springs used in the 2D ANSYS analyses, and thus addresses the concern regarding the calculation of soil bearing pressure demand. However, for the design of the basemat, Westinghouse has not demonstrated that its use of uniform Winkler type soil springs is adequate. As noted in the prior RAI, due to the Boussinesq effect in soil, the distribution of stiffness would be higher at the edges and lower away from the edges. Therefore, Westinghouse is requested to demonstrate that the use of the uniform soil springs for the design of the foundation is acceptable, when it is known that the actual distribution of the soil stiffness would not be uniform.

Additional Request (Revision 3):
NRC Meeting August 10-14

1. Clarify the Model identification in Table RAI-TR85-SEB1-32-1, Line 2 and Line 3. Consider use of description in Appendix 3G.
2. In the second paragraph on page 4 of 13 of the RAI response how does the referenced report from section 2.7.2 of TR85 demonstrate the acceptability of using Winkler springs instead of the method using Boussinesq effect.

Additional Request (Revision 4):

The staff reviewed the Westinghouse response to RAI-TR85-SEB1-32, Rev. 3 and determined that Item 2 of the response did not adequately address staff's concerns. The information provided does not clearly demonstrate that the bending moments and shear forces in the basemat using the Winkler soil springs are acceptable. For example, as shown in Figures RAI-TR85-SEB1-32-2 and 3 provided in Revision 2 to this RAI, there are locations where the bending moments using the finite element model are larger than the results for the Winkler soil spring model. Therefore, provide the technical basis for using the Winkler soil spring model. The technical basis should include tabulated or plotted curves (not contour plots) showing moments (positive and negative) and shear forces at locations in the basemat that govern the design for the rest of basemat.

Additional Request (Revision 5):

The staff reviewed the response provided in Westinghouse letter dated July 30, 2010 and determined that the following items need to be addressed:

(1) Correct the typo of "4861%" in the second paragraph on Page 7 of 20 of the response.

(2) Explain why the required reinforcement went up from 1.87 in^2/ft to 2.00 in^2/ft from the prior RAI submittal.

(3) In order to justify the use of 20% moment redistribution, provide information which demonstrates that the provisions in Section 8.4 of ACI 349 have been satisfied.

(4) Even with the redistribution of 20% negative moment, the reinforcement design still does not meet code requirements. From the descriptive information provided in the last two paragraphs of Page 7 of 20, it is not evident that the 5% exceedance of code limits is acceptable. Rather than justify potential conservations in the design, it is preferable to show that the provided reinforcement is greater than the calculated required reinforcement.

(5) Provide the comparison for the WEC 100/40/40 method versus the ASCE 4-98 method. The NRC updated version of the Path Forward document transmitted to WEC required this comparison as stated below:

" Include a table that compares 16 cases with maximum reinforcement required and maximum member forces used in design to the maximum maximum member forces and corresponding maximum reinforcement required based on the ASCE 4-98 approach in order to show that the differences in the application of 100-40-40 is negligible for the basemat."

(6) On Page 11 of 20, explain for (a) LC06 versus LC07 and (b) LC09 versus LC14, why higher moments MX result in lower required steel AXBOT.

(7) As identified in the Path Forward document, under RAI-SRP-3.8.3-SEB1-03, WEC was requested to demonstrate that there are no significant increases in the basemat forces due to the issue of concrete cracking. If the cracking of the NI increases the loads to the basemat, then this effect should be included in the basemat design.

Westinghouse Response:

Subsection 2.5.4.2 is being revised to clarify the maximum bearing pressure of 35 ksf, as stated in the DCD, it is obtained from analyses using uniform soil springs. The revision now indicates the line of lift off, thereby defining the maximum total load applied to the foundation at the time of maximum demand. Unlike the static case, where the allowable bearing capacity is controlled by settlements, the dynamic bearing capacity is related to the overall loading on the foundation and to the shear strength mobilized over a failure surface in the foundation soils. The local maximum values close to the edge are not significant to this capacity and will redistribute if local stresses in the soil are excessive. This total load rather than a peak stress below an edge is to be considered by the Combined License applicant in demonstrating stability of the foundation material.

Various analyses described in the report investigate the effect of modeling the soil with uniform spring and solid element representations. Comparisons are made in linear analyses using SASSI and ANSYS. Comparisons are made in ANSYS linear and non-linear analyses to show the effect of lift off. The analyses show small differences in the distribution of the bearing pressures but good agreement in the total loads imposed on the foundation material. The small differences in distribution (the Boussinesq effect) are not significant to the evaluation of the stability of the foundation material.

Westinghouse Response (Revision 1):

The maximum seismic bearing pressure demand defined for comparison to the subgrade pressure capacity is consistent with the DCD. See RAI-TR85-SEB1-03, Rev. 1 for discussion of the 35 ksf maximum bearing seismic demand.

In response to the many questions in this and other RAIs, Westinghouse has revised the basis for the bearing demand. The demand is now based on 3D SASSI analyses using the 3D NI20 finite element model as described in the response to RAI-TR85-SEB1-03, Rev 1. This change to use of the 3D SASSI results addresses the original question in this RAI. The additional questions in Rev 1 of this RAI apply to the Rev 0 response which has now been superseded.

The statement in the DCD Section 2.5.4.2, "The evaluation may be limited to response in the east-west direction since the bearing demand is lower in the north-south direction" has been removed. See DCD revision section below.

Westinghouse Response (Revision 2):

Table RAI-TR85-SEB1-32-1 shows the summary of the maximum reactions of the nuclear island for various soil and analysis methods. The results from Table 2.4-5 of the technical report, APP-GW-GLR-044, R1 (TR85), are shown for Item 1. Two other sources are contained in the table as comparison. The results of the linear analyses show consistent results demonstrating that the equivalent static analyses of the basemat result in bearing pressures similar to a more realistic model represented in the 3D SASSI analyses presented in Table 2.4-5.

Section 2.7.1 of the technical report describes studies performed to evaluate the effect of different soil modeling. These studies analyzed a 3D finite element model of the complete nuclear island on soil finite elements or soil springs. Additional comparisons are provided in this response for the following soil models:

- Winkler soil springs of 520 kcf similar to the design analyses of the basemat (Model W)
- Finite element model of 80-foot deep soil layer below the nuclear island. The properties for this soil were selected to match the 520 kcf soil (Model L080).

Figure RAI-TR85-SEB1-32-1 shows bearing pressures due to dead load. The sections are located as shown in Figure 2.7-2 of the technical report. The RAI figure only shows the two cases identified above. The finite element soil model shows high local bearing pressures close to the edge. This is due to the Boussinesq effect. The higher pressures at the edge result in lower pressures away from the edge. Figures RAI-TR85-SEB1-32-2 and 3 show bending moment contours MX and MY for these two cases. It is seen that the bending moments for the soil spring case are higher than those for the soil finite element model even in the bays immediately adjacent to the edge. ~~The 100-40-40 method as applied by Westinghouse can be further shown to be conservative by comparing the bearing press~~

Section 2.7.2 of the technical report describes an additional study performed to evaluate the basemat soil interaction. The north-west corner of the AP1000 shown in Figure RAI-TR85-SEB1-32-4 was modeled and analyzed in two dimensions using the non-linear VECTOR2 structural analysis program. The model of the basemat and soil is shown in Figure RAI-TR85-SEB1-32-5. The model of the basemat is 20269.2 mm (66.5') long, simulating 3 bays of 18' and ½ bay of 25', and 1828.8 mm (6') high. The element size is 152.4 mm (6") x 304.8 mm (12") for the first 55' and 152.4 mm (6") x 292.1 mm (11.5") for the last 11.5'. The total number of nodes and elements for the basemat is 884 and 804, respectively. The model of the soil is 23104.8 mm (75.8' depth) and 61069.2 mm (200.3'). The soil model extends almost twice the soil depth beyond the end of the basemat. The total number of nodes and elements for the soil is 4794 and 4642, respectively. The soil properties are chosen to give the same vertical displacement of the nuclear island under dead load as the 520 kcf soil springs. X-direction is horizontal and Y is

vertical. The nodes on the last column are restrained in the X-direction to simulate symmetry. The VECTOR2 program considers cracking of the concrete and non-linear behavior of the reinforcement. Structural response is calculated up to failure for monotonically applied vertical displacement of the shear walls. Contact pressures on the soil are shown in Figure RAI-TR85-SEB1-32-6 (Figure 2.7-10, TR85) as a function of the applied displacement. They indicate substantial Boussinesq effect with high bearing pressures below the edge of the basemat. The analyses showed significant redistribution of soil bearing pressures as the load increased. The basemat withstood loading about three and a half times the design loads with final failure occurring in shear close to the exterior wall.

The studies documented in section 2.7 of the technical report and summarized above show the Boussinesq effect in rock and soil with an effective stiffness that is higher at the edges and lower away from the edges. This distribution is presented on Figure RAI-TR85-SEB1-32-7. The influence values represent the effect of the contact on a half space beneath a rigid circular footing. The Boussinesq equation does not account for the influence of the basemat's embedment depth of 39.5 feet which would increase the bearing capacity of the foundation. Because of the basemat dimensions (plan and thickness), the foundation would be considered flexible. The studies demonstrate that the use of uniform Winkler type soil springs is adequate for a flexible mat foundation.

Westinghouse Response (Revision 3):

1. The 2D SASSI model listed at Line 2 of Table RAI-TR85-SEB1-32-1 refers to the East-West 2D stick model described in section 2.4.1 of APP-GW-GLR-044, and also shown in Figure 2.4-2 of that report. The 2D Time History model listed at Line 3 of the table refers to the lift-off analysis performed in ANSYS described in section 2.4.2 of APP-GW-GLR-044, and shown in Figure 2.4-4 of that report.

2. The referenced report, from section 2.7.1 of TR85, demonstrates the acceptability of using Winkler springs instead of the method using Boussinesq effect. As concluded in section 2.7.1.2.4, the analyses with finite element models of the soil were performed as linear elastic analyses. They require much greater computer running time and do not lead to significantly better results. The design analyses are non-linear to consider lift off. They require a more detailed model of the nuclear island than that used in the studies. They must address more combinations of seismic input than used in the studies. Hence Winkler springs were selected for use in the design analyses similar to those used in the AP600 analyses.

   As discussed in section 2.7.1.2.1, the models with finite element representation of the soils show larger bearing reactions at the edges than the Winkler spring model. These higher reactions at the edges give a corresponding reduction of bearing reactions and member forces away from the edges. Hence the uniform Winkler

springs are conservative for design of the basemat since reinforcement in the basemat is controlled by member forces below the center of each panel and the interior walls (the exterior wall acts more like a simple support than a fixed support).

The referenced report from section 2.7.2 of TR85 does not directly demonstrate the acceptability of using Winkler springs instead of the method using Boussinesq effect. However, it shows substantial margin (about three and a half times the design loads) in the design with a more detailed soil and structure model that also shows bearing pressures consistent with the Boussinesq distribution.

Westinghouse Response (Revision 4):

Moments (positive and negative) and shear forces are shown in Table RAI-TR85-SEB1-32-2 in elements in the middle of the two critical sections identified in the DCD. The element locations are shown in Figure RAI-TR85-SEB1-32-8. Positive moments put the top surface of the mat in tension. The critical sections were selected as representative of the most limiting portions of the basemat and are described in DCD subsection 3.8.5.4.4 as follows:

Basemat between column lines 9.1 and 11 and column lines K and L (Bay 2 in Table)

This portion of the basemat is designed as a two way slab with the shorter directions spanning a distance of 23′ 6″ between the walls on column lines K and L. The slab is continuous with the adjacent slabs to the east and west. The critical loading is the bearing pressure on the underside of the slab due to dead and seismic loads. This establishes the demand for the top flexural reinforcement at mid span and for the bottom flexural and shear reinforcement at the walls. The basemat is designed for the member forces from the analyses described in subsection 3.8.5.4.1. The top and bottom reinforcement in the east west direction of span are equal. The reinforcement provided is shown in sheets 1, 2 and 5 of Figure 3.8.5-3. Typical reinforcement details showing use of headed reinforcement for shear reinforcement are shown in Figure 3H.5-3.

Basemat between column lines 1 and 2 and column lines K-2 and N (Bay 1 in Table)

This portion of the basemat is designed as a two way slab with the shorter direction spanning a distance of 22′ 0″ between the walls on column lines 1 and 2. The slab is continuous with the adjacent slabs to the north and with the exterior wall to the south. The critical loading is the bearing pressure on the underside of the slab due to dead and seismic loads. This establishes the demand for the top flexural reinforcement at mid span and for the bottom flexural and shear reinforcement at wall 2. The basemat is designed for the member forces from the analyses on uniform soil springs described in subsection 3.8.5.4.1. The reinforcement provided is shown in sheets 1, 2 and 5 of Figure 3.8.5-3. Typical reinforcement details showing use of headed reinforcement for shear reinforcement are shown in Figure 3H.5-3.

Table RAI-TR85-SEB1-32-2 shows the bending moments and shear forces in the principal span direction (X direction for Bay 1 and Y direction for Bay 2). Bay 2 is away from the edges of the basemat. The maximum positive moment and shear forces in Bay 2 are lower with the soil

model (L-080) than the Winkler spring model. The minimum (maximum negative) moment is about equal with the soil model (L-080) and the Winkler spring model.

Bay 1 is at the south west corner of the basemat. In this bay the maximum positive moment and shear forces are also lower with the soil model (L-080) than the Winkler spring model. The mid span positive moment reduces by 45%. However, the minimum (maximum negative) moment with the soil model (L-080) is 48~~61~~% greater than the Winkler spring model. This increase was evaluated as follows:

> The bottom reinforcement provided in Bay 1 in the north south direction is #14 bars at 12" centers as shown in Table 2.6.9 of the TR85 report. This provides an area of 2.25 in^2/ft. The design calculation shows that the reinforcement required in the highest loaded element at this location is 2.00 in^2/ft. This demand is calculated for the design loads and includes the additional 20% margin described in section 2.6.2 of the report. The governing load case is Load Case 3-6 (Es= -1.0xSns+0.4xSew-0.4xSvt) which maximizes the bearing pressure in the south-west corner. An increase in the demand by 48% would increase the reinforcement required to 2.96 in^2/ft which is 32% greater than that provided. The ACI Code permits redistribution of negative and positive moments by up to 20% for a flexural member with equal top and bottom reinforcement. The slab has a clear span of 19' in the north-south direction and 40' in the east-west direction so the moment at the section shown in Table RAI-TR85-SEB1-32-2 is behaving similar to a one way flexural member. Since the mid span moment reduces by 45% in the L-080 model, and the required positive reinforcement based on the design analyses is also less than the reinforcement provided, 20% of the negative moment can be redistributed. Thus, the reinforcement required for the negative moment at the end span is 0.8 x 2.96 = 2.37 in^2/ft, which is 5% greater than that provided.
>
> The bearing reactions from the equivalent static non-linear lift off analyses of the basemat are conservative relative to the linear elastic SASSI analyses which show that the lift off is negligible. This conservatism is shown in Tables 2.6.2 (c) and (d) of TR 85 showing that the non-linear lift off analyses are 20% higher at the south west corner than the results of analyses with input enveloping all the soil cases (33.1 ksf versus 27.1 ksf).
>
> The L080 soil model has relatively large element sizes for the soil below the edge of the nuclear island. This would be expected to overestimate the soil stiffness below the edge of the nuclear island thus overestimating the Boussinesq effect. Even if the member forces were to be amplified by 48% shown in the comparison study of the two models, the span has sufficient margin to accommodate the greater negative moment demand shown by the L080 soil model.

A detailed study of the south-west bay on soil was also performed using the non-linear Vector analysis methodology similar to that described for the north end of the nuclear island in section 2.7.2 of the report. In these 2D analyses the soil was represented by a much more detailed model than was possible in the 3D L-080 model. The results of this analysis are shown below in

the same format as that in Table 2.7-2 of the report for the north portion. This shows a significantly increased capacity for the south west bay when analyzed in the detailed Vector 2 analyses relative to the Winkler soil spring case (100 ksf versus 41 ksf).

Table 6.2: Summary of results for VECTOR2 SW runs

Run ID	Elastic limit	Initial strain hardening[*]							90 % of ultimate[**]						
	Average Contact pressure	Average Contact Pressure	Max. Contact Pressure	Min. Contact Pressure	Support Displ.	Max. Vert. Def.	Max. Horiz. Def.	Max. Crack size	Average Contact Pressure	Max. Contact Pressure	Min. Contact Pressure	Support Displ.	Max. Vertical Def.	Max. Horiz. Def.	Max. Crack size
SWUDL	0.53 Mpa (11 Ksf)	1.30Mpa (27 Ksf)	N/A	N/A	N/A	5.3 mm (0.21in)	2.6 mm (0.10in)	2.2 mm (0.09in)	1.72Mpa (36 Ksf)	N/A	N/A	N/A	12.2mm (0.48in)	6.6 mm (0.26in)	6.1 mm (0.24in)
SWSPR	0.53 Mpa (11 Ksf)	1.44Mpa (30 Ksf)	1.91Mpa (40 Ksf)	1.34Mpa (28 Ksf)	20.3mm (0.8 in)	5.4 mm (0.22in)	2.7 mm (0.11in)	2.4 mm (0.09in)	2.0 Mpa (41 Ksf)	2.96Mpa (62 Ksf)	1.72Mpa (36 Ksf)	30.6mm (1.2 in)	11.0mm (0.47in)	6.5 mm (0.26in)	5.8 mm (0.23in)
SWHALFSP	0.72 Mpa (15 Ksf)	Same as 90 % of ultimate							4.8 Mpa (100Ksf)	11.0Mpa (230Ksf)	2.0 Mpa (42 Ksf)	61.0mm (2.4 in)	9.4 mm (0.37in)	2.2 mm (0.09in)	2.3 mm (0.09in)

Thus, the increase in negative moments showing up in the L-080 model analyses do not affect the overall strength of the nuclear island basemat. The analyses using the Winkler springs provide a design with substantial margin for the design loading.

The two critical bays were selected in the AP600 design certification to demonstrate design methodology. They include a bay with maximum span between the shear walls and a bay at the edge with maximum span and maximum bearing demand. These bays bound the results for other bays. The bottom reinforcement in both directions is uniform (#14 bars at 12" centers each way). Other bays have the same reinforcement and lower demand so similar amplification of the negative moment demand (tension on the bottom face) would be within the reinforcement provided.

The analyses are non-linear analyses performed using 16 combinations (1.0 on horizontal input) of the 100/40/40 equivalent static seismic directions of input. The other 8 combinations (1.0 on vertical input) have been shown not to govern (see response to RAI-TR85-SEB1-27). Each of the 16 combinations results in maximum bearing reactions below a different part of the basemat. Bearing reactions for representative cases are shown in Figures 2.6.4 to 2.6-8 in the TR85 report. For each analysis member forces are combined following the ACI Code equations to develop the required reinforcement in each direction. An example of the member forces in a critical element, TX, TXY, and MX and the required reinforcement, AXTOP and AXBOT is shown in Table RAI-TR85-SEB1-32-3. These are the member forces that affect the reinforcement demand in the north south direction. The reinforcement demand is primarily associated with the bending moment MX which is largest in cases LC06 and LC07 with the seismic input towards the south. The reinforcement demand from the 16 cases is enveloped.

Westinghouse Response (Revision 5):

(1) The typo of "4861%" in the second paragraph on Page 7 of 20 of the response.(now at the top of page 8) has been corrected to 48%.

(2) -A detailed review of FE results showed that the previous response did not use the element with the maximum reinforcement demand. The ~~old~~previous results were for element 3831 and the new results are for element 3835 as marked below on the finite element model of this bay. The average demand for the four elements in the middle part of the bay (3831, 3833, 3835 and 3837) is 1.91 in^2/ft. When averaged over six elements (these four elements plus the adjacent elements) the average demand is 1.81 in^2/ft.

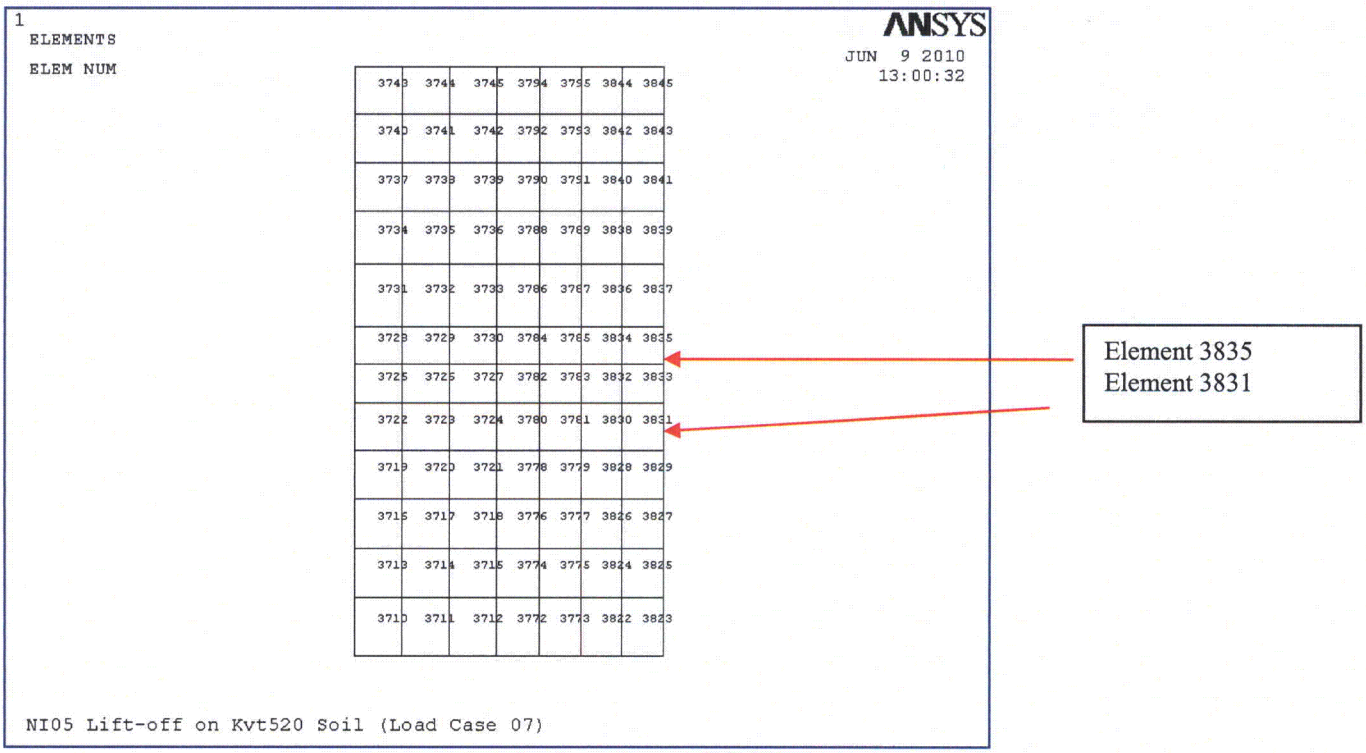

(3) Section 8.4 of ACI 349 states:

8.4—Redistribution of negative moments in continuous nonprestressed flexural members

8.4.1 Except where approximate values for moments are used, it shall be permitted to increase or decrease negative moments calculated by elastic theory at supports of continuous flexural members for any assumed loading arrangement by not more than $20\,(1-(\rho-\rho')/\rho_b)$

8.4.2 The modified negative moments shall be used for calculating moments at sections within the spans.

8.4.3 Redistribution of negative moments shall be made only when the section, at which moment is reduced, is so designed that ρ or $(\rho - \rho')$ is not greater than $0.50\ \rho_b$, where

$$\rho_b = 0.85\beta_1 f_c'/f_y \quad 87,000/(87,000 + f_y)$$

The negative moment occurs in a continuous span of the basemat below the wall on column line 2 as shown in Figure RAI-TR85-SEB1-32-8. Both the top and bottom reinforcement in the north south direction is #14 bars at 12" centers giving $\rho = \rho' = 0.003$. The balanced reinforcement, ρ_b, = 0.034. Thus, $\rho - \rho' = 0$ and paragraphs 8.4.1 and 8.4.3 permits a redistribution of negative moments equal to 20%. As described the mid-span moments are well below the design strength and are able to accommodate this redistribution described in paragraph 8.4.2.

(4) As described in the response to item (2), the demand averaged over 4 elements is 1.91in^2/ft and is 1.81in^2/ft when averaged over 6 elements. ACI 349 permits use of demand based on yield line analyses in paragraph 13.15. A typical yield line pattern would have a line of rotation along the mid length of the wall on column line 2. Averaging over 6 elements is about one half the length of the slab and about three times the slab thickness. This would reduce the demand from 2.0 to 1.81 in^2/ft (a 10% reduction). Thus, averaging of the results from the elastic analyses would show the design satisfying the code strength requirement.

As described in the RAI-TR85-SEB1-32 Revision 4 response, "The bearing reactions from the equivalent static non-linear lift off analyses of the basemat are conservative relative to the linear elastic SASSI analyses which show that the lift off is negligible. This conservatism is shown in Tables 2.6.2 (c) and (d) of TR 85 showing that the non-linear lift off analyses are 20% higher at the south west corner than the results of analyses with input enveloping all the soil cases (33.1 ksf versus 27.1 ksf)." This represents a further reduction in demand of 20% providing additional assurance that the provided reinforcement is greater than the calculated required reinforcement.

As described in the RAI-TR85-SEB1-32 Revision 4 response, the detailed study of the south-west bay on soil performed using the non-linear Vector analysis methodology showed large margin in the capacity of this bay.

The design methodology includes many conservatisms as described in the preceding paragraphs, thus assuring a safe design

(5) ASCE 4-98 does not provide guidance for combining member forces for the 100-40-40 method. ASCE 4-98 does provide a method for use with response spectrum results, but acknowledges that it is conservative. However, this method is not applicable in non-linear analyses

Table RAI-TR85-SEB1-32-3 shows the absolute value of the member forces from the 17 load combinations. Subsequent rows show combinations of member forces requested to be evaluated by the NRC staff in which each seismic member force takes a positive or negative sign. The first row assumes all member forces are positive (tension is positive); together with the other rows there are 8 cases giving all sign combinations for the seismic member forces. The reinforcement required for each of these combinations of member forces is shown. The required reinforcement with these conservative assumptions is 3.47 in^2/ft compared with the 2.0 in^2/ft from the envelope of the non-linear analyses. The difference is primarily in the assumption that the axial force is tension instead of compression. For the controlling load cases the basemat is in compression since the horizontal resistance only occurs below the portion of the basemat that does not lift off (see Figure 2.6-5 of the TR85 basemat report for the bearing pressures for LC (6)). Hence the assumption of the maximum tension concurrent with the maximum bending moment (and bearing reaction) is not realistic. The table also shows a higher demand for the top reinforcement due to the arbitrary assumption that the moment may be positive at this support. This is not possible since the bearing pressure can only be compression.

Tables RAI-TR85-SEB1-32-4 ~~to~~through RAI-TR85-SEB1-32-7 shows the member forces for four additional elements. The location of these elements is shown in Figure ~~Table R~~RAI-TR85-SEB1-32-9.

(6) In Table RAI-TR85-SEB1-32-3, there are cases where higher moments MX result in lower required steel AXBOT. This is due to the axial compression.

(7) Member forces in the basemat are calculated using the maximum ZPAs of the CSDRS. Figure RAI-TR85-SEB1-32-10 provides an FRS comparison between the linear 80% stiffness and the non-linear ABAQUS models at the top of the Shield Building and Auxiliary Building. The FRS results from analyses with the non-linear materials include the effect of cracking in the concrete and SC elements. The ZPAs obtained from the non-linear analyses was either the same or lower than the ZPAs obtained from the 0.8 Em linear analyses. Thus, the use of 80% stiffness is an appropriate approach to calculating basemat member forces. Additional information is provided in the response to RAI SRP3.7.1-SEB1-19.

(8) Table RAI-TR85-SEB1-32-1 shows the summary of the maximum reactions of the nuclear island for various soil and analysis methods. In Figure RAI-TR85-SEB1-32-11 a comparison between equivalent static and dynamic time history analyses is made. Both linear and nonlinear models are compared. The upper figure shows linear results and the lower figure shows non-linear results. In linear analysis, the differences between dynamic and static displacements are small. However, in non-linear, those differences are larger. This results in a smaller contact area and larger bearing stresses. Thus for the hard rock case the 1.0EW-0.4VT case results in a bearing pressure of 47.1 ksf, which is larger than

the 34.9 ksf obtained from the dynamic results. This shows the conservatism in the equivalent static method applied for the basemat design.

Table RAI-TR85-SEB1-32-1

Maximum Basemat Bearing Pressure (Summary)

No.	Method of Analysis	Foundation Conditions					
		HR (ksf)	FR (ksf)	SR (ksf)	UBSM (ksf)	SM (ksf)	SS (ksf)
1	3D SASSI, NI20 Model, TH + vertical earthquake	35.0 *	27.9	24.0	25.7	23.1	21.9
2	2D SASSI, ni2D** model	29.1	24.0	24.5	27.4	30.2	20.2
3	2D ANSYS Time History, ni2D** model: Linear	32.8	N/A	N/A	31.7	30.8	N/A
	:Lift off	34.9	N/A	N/A	33.5	32.2	N/A
4	2D ANSYS Equivalent Static 100/40, ni2D** Lift off model	47.1	N/A	N/A	N/A	N/A	N/A

Notes:

* 38.3 ksf was the maximum localized peak calculated; a limit of 35 ksf for maximum bearing seismic demand is obtained by averaging the soil pressure about the West edge of the shield building where the maximum stress occurs.

** The ni2D model refers to the East-West 2D stick model of the Nuclear Island used for the SASSI and ANSYS analyses. The SASSI analysis used the model embedded in soil 120' below grade. The ANSYS linear lift off model was a non-linear analysis on a rigid basemat. The SASSI and ANSYS model representations are shown in TR85, Figures 2.4-2 and 2.4-4 respectively.

Table RAI-TR85-SEB1-32-2
Bending Moments and Shears in Critical Elements

	Model W		Model L-080		Ratio	L-080/W
ELEM	MX	NX	MX	NX	MX	NX
Bay 1	kip.ft/ft	kip/ft	kip.ft/ft	kip/ft		
427	148.73	38.44	104.65	18.58	0.70	0.48
428	146.25	39.52	107.74	21.23	0.74	0.54
442	248.89	-31.84	123.03	-27.65	0.49	0.87
443	251.95	-29.42	137.34	-27.28	0.55	0.93
457	-93.01	-84.24	-137.56	-59.28	1.48	0.70
458	-83.81	-86.78	-134.98	-65.96	1.61	0.76
Max	251.95	39.52	137.34	21.23	0.55	0.54
Min	-93.01	-86.78	-137.56	-65.96	1.48	0.76
	MY	NY	MY	NY	MY	NY
Bay 2	kip.ft/ft	kip/ft	kip.ft/ft	kip/ft		
776	-69.67	45.92	-65.82	20.64	0.94	0.45
777	46.23	29.80	8.29	23.66	0.18	0.79
778	129.31	7.58	70.40	4.09	0.54	0.54
779	128.48	-13.64	68.83	-8.04	0.54	0.59
780	-32.80	-39.68	-35.86	-25.98	1.09	0.65
795	-66.58	43.90	-70.83	23.01	1.06	0.52
796	43.55	29.44	7.87	24.90	0.18	0.85
797	121.48	7.19	73.49	4.58	0.60	0.64
798	120.12	-14.14	72.31	-9.36	0.60	0.66
799	-26.55	-37.40	-33.09	-26.88	1.25	0.72
Max	129.31	45.92	73.49	24.90	0.57	0.54
Min	-69.67	-39.68	-70.83	-26.88	1.02	0.68

Note: See Figure RAI-TR85-SEB1-32-8 for location of elements

Table RAI-TR85-SEB1-32-~~32~~
Design Member Forces and Required Reinforcement in Critical Element

Element	3835										
	D	L	Ens	Eew	Ev	TX	TXY	MX	AXTOP	AXBOT	AXYSH
LC01	1.4	1.7				-7.7	-7.9	-344.8	1.307	1.595	0.000
LC02	1.0	1.0	1.0	0.4	0.4	-31.3	-13.8	103.5	1.307	1.595	0.000
LC03	1.0	1.0	1.0	0.4	-0.4	57.0	44.6	58.8	1.307	1.595	0.000
LC04	1.0	1.0	1.0	-0.4	0.4	-8.8	7.2	79.8	1.307	1.595	0.000
LC05	1.0	1.0	1.0	-0.4	-0.4	-2.4	25.2	104.5	1.307	1.595	0.000
LC06	1.0	1.0	-1.0	0.4	0.4	-103.6	-8.2	-752.3	1.307	1.866	0.000
LC07	1.0	1.0	-1.0	0.4	-0.4	-77.8	-8.8	-738.6	1.307	1.996	0.000
LC08	1.0	1.0	-1.0	-0.4	0.4	-83.9	-67.9	-579.8	1.307	1.663	0.000
LC09	1.0	1.0	-1.0	-0.4	-0.4	-72.7	-61.7	-631.7	1.307	1.663	0.000
LC10	1.0	1.0	0.4	1.0	0.4	23.5	64.6	-1.8	1.307	1.595	0.000
LC11	1.0	1.0	0.4	1.0	-0.4	26.8	82.5	-198.2	1.307	1.595	0.000
LC12	1.0	1.0	0.4	-1.0	0.4	4.3	-9.2	52.1	1.307	1.595	0.000
LC13	1.0	1.0	0.4	-1.0	-0.4	14.8	-40.3	-6.5	1.307	1.595	0.000
LC14	1.0	1.0	-0.4	1.0	0.4	-59.2	116.7	-529.7	1.307	1.866	0.102
LC15	1.0	1.0	-0.4	1.0	-0.4	-45.3	70.2	-599.0	1.307	1.866	0.000
LC16	1.0	1.0	-0.4	-1.0	0.4	-47.7	-96.6	-219.8	1.307	1.595	0.000
LC17	1.0	1.0	-0.4	-1.0	-0.4	-36.8	-84.4	-326.9	1.307	1.595	0.000

NRC Staff Requested Methodology	TX	TXY	MX	AXTOP	AXBOT	AXYSH
Maximum absolute value	92.7	116.7	259.8	1.866	1.595	0.493
	92.7	116.7	-752.3	1.307	3.474	0.493
Other combinations with	92.7	-128.0	259.8	1.866	1.595	0.715
opposite signs for seismic	92.7	-128.0	-752.3	1.307	3.474	0.715
	-103.6	116.7	259.8	1.307	1.595	0.102
	-103.6	116.7	-752.3	1.307	1.866	0.102
	-103.6	-128.0	259.8	1.307	1.595	0.324
	-103.6	-128.0	-752.3	1.307	1.866	0.324

Note: Sign of seismic member forces only are taken as plus and minus.

Table RAI-TR85-SEB1-32-4
Design Member Forces and Required Reinforcement in Critical Element

Element 3688

	D	L	Ens	Eew	Ev	TX	TXY	MX	AXTOP	AXBOT	AXYSH
LC01	1.4	1.7				-6.6	1.0	362.0	1.555	1.595	0.000
LC02	1.0	1.0	1.0	0.4	0.4	-4.3	-4.5	-58.7	1.307	1.595	0.000
LC03	1.0	1.0	1.0	0.4	-0.4	0.3	-17.8	-74.1	1.307	1.595	0.000
LC04	1.0	1.0	1.0	-0.4	0.4	12.4	15.0	-22.6	1.307	1.595	0.000
LC05	1.0	1.0	1.0	-0.4	-0.4	21.0	0.7	94.8	1.307	1.595	0.000
LC06	1.0	1.0	-1.0	0.4	0.4	-42.2	-5.3	450.7	1.547	1.595	0.000
LC07	1.0	1.0	-1.0	0.4	-0.4	-34.4	-2.3	487.9	1.824	1.595	0.000
LC08	1.0	1.0	-1.0	-0.4	0.4	-43.2	-2.1	647.6	1.870	1.595	0.000
LC09	1.0	1.0	-1.0	-0.4	-0.4	-39.5	-1.0	687.1	2.028	1.595	0.000
LC10	1.0	1.0	0.4	1.0	0.4	-2.2	8.1	-56.9	1.307	1.595	0.000
LC11	1.0	1.0	0.4	1.0	-0.4	5.8	-4.8	-70.1	1.307	1.595	0.000
LC12	1.0	1.0	0.4	-1.0	0.4	3.3	4.1	345.2	1.762	1.595	0.000
LC13	1.0	1.0	0.4	-1.0	-0.4	-2.9	3.7	434.3	1.866	1.595	0.000
LC14	1.0	1.0	-0.4	1.0	0.4	5.1	4.5	-55.3	1.307	1.595	0.000
LC15	1.0	1.0	-0.4	1.0	-0.4	-9.2	13.2	60.8	1.307	1.595	0.000
LC16	1.0	1.0	-0.4	-1.0	0.4	-36.1	0.6	706.7	2.226	1.595	0.000
LC17	1.0	1.0	-0.4	-1.0	-0.4	-28.6	0.4	678.2	2.149	1.595	0.000

Table RAI-TR85-SEB1-32-5
Design Member Forces and Required Reinforcement in Critical Element

Element	4714										
	D	L	Ens	Eew	Ev	TX	TXY	MX	AXTOP	AXBOT	AXYSH
LC01	1.4	1.7				-3.4	-10.8	78.3	1.307	1.595	0.000
LC02	1.0	1.0	1.0	0.4	0.4	-20.9	-32.8	89.5	1.307	1.595	0.000
LC03	1.0	1.0	1.0	0.4	-0.4	-15.9	-34.1	102.6	1.307	1.595	0.000
LC04	1.0	1.0	1.0	-0.4	0.4	-80.2	-54.1	230.6	1.307	1.595	0.000
LC05	1.0	1.0	1.0	-0.4	-0.4	-71.0	-54.3	233.2	1.307	1.595	0.000
LC06	1.0	1.0	-1.0	0.4	0.4	3.9	26.9	-34.4	1.307	1.595	0.000
LC07	1.0	1.0	-1.0	0.4	-0.4	12.0	29.6	-45.7	1.307	1.595	0.000
LC08	1.0	1.0	-1.0	-0.4	0.4	5.4	17.4	-18.3	1.307	1.595	0.000
LC09	1.0	1.0	-1.0	-0.4	-0.4	16.6	18.4	16.5	1.307	1.595	0.000
LC10	1.0	1.0	0.4	1.0	0.4	25.7	10.7	-36.1	1.307	1.595	0.000
LC11	1.0	1.0	0.4	1.0	-0.4	49.0	3.3	-52.1	1.307	1.595	0.000
LC12	1.0	1.0	0.4	-1.0	0.4	-128.3	-53.3	320.2	1.307	1.595	0.000
LC13	1.0	1.0	0.4	-1.0	-0.4	-93.8	-48.6	277.8	1.307	1.595	0.000
LC14	1.0	1.0	-0.4	1.0	0.4	-8.9	17.4	-30.4	1.307	1.595	0.000
LC15	1.0	1.0	-0.4	1.0	-0.4	14.7	19.6	-43.5	1.307	1.595	0.000
LC16	1.0	1.0	-0.4	-1.0	0.4	-65.8	-13.1	193.7	1.307	1.595	0.000
LC17	1.0	1.0	-0.4	-1.0	-0.4	-56.2	-20.2	186.7	1.307	1.595	0.000

For this bay the calculated demand is less than the minimum required reinforcement.

Table RAI-TR85-SEB1-32-6
Design Member Forces and Required Reinforcement in Critical Element

Element 4856

	D	L	Ens	Eew	Ev	TX	TXY	MX	AXTOP	AXBOT	AXYSH
LC01	1.4	1.7				-7.2	6.4	184.7	1.307	1.595	0.000
LC02	1.0	1.0	1.0	0.4	0.4	-40.4	26.0	305.8	1.307	1.595	0.000
LC03	1.0	1.0	1.0	0.4	-0.4	-34.7	26.0	334.7	1.307	1.595	0.000
LC04	1.0	1.0	1.0	-0.4	0.4	-40.3	-10.8	358.7	1.393	1.595	0.000
LC05	1.0	1.0	1.0	-0.4	-0.4	-35.7	-9.6	383.0	1.578	1.595	0.000
LC06	1.0	1.0	-1.0	0.4	0.4	-9.6	31.8	-40.1	1.307	1.595	0.000
LC07	1.0	1.0	-1.0	0.4	-0.4	-10.1	47.8	-58.4	1.307	1.595	0.000
LC08	1.0	1.0	-1.0	-0.4	0.4	-6.1	-7.4	-47.0	1.307	1.595	0.000
LC09	1.0	1.0	-1.0	-0.4	-0.4	-0.6	-19.9	-48.9	1.307	1.595	0.000
LC10	1.0	1.0	0.4	1.0	0.4	-1.3	-1.5	-28.9	1.307	1.595	0.000
LC11	1.0	1.0	0.4	1.0	-0.4	-14.2	41.8	133.7	1.307	1.595	0.000
LC12	1.0	1.0	0.4	-1.0	0.4	-22.1	-58.7	271.2	1.342	1.595	0.000
LC13	1.0	1.0	0.4	-1.0	-0.4	-19.5	-39.8	297.1	1.460	1.595	0.000
LC14	1.0	1.0	-0.4	1.0	0.4	-0.3	5.7	-44.3	1.307	1.595	0.000
LC15	1.0	1.0	-0.4	1.0	-0.4	13.8	44.2	-66.6	1.307	1.595	0.000
LC16	1.0	1.0	-0.4	-1.0	0.4	20.2	-62.1	-13.8	1.307	1.595	0.000
LC17	1.0	1.0	-0.4	-1.0	-0.4	8.8	-44.1	112.9	1.307	1.595	0.000

Table RAI-TR85-SEB1-32-7
Design Member Forces and Required Reinforcement in Critical Element

Element	4886										
	D	L	Ens	Eew	Ev	TX	TXY	MX	AXTOP	AXBOT	AXYSH
LC01	1.4	1.7				-7.3	14.7	148.4	1.307	1.595	0.000
LC02	1.0	1.0	1.0	0.4	0.4	-43.9	47.3	325.1	1.399	1.595	0.000
LC03	1.0	1.0	1.0	0.4	-0.4	-37.2	48.9	348.1	1.644	1.595	0.000
LC04	1.0	1.0	1.0	-0.4	0.4	-6.4	38.3	212.8	1.307	1.595	0.000
LC05	1.0	1.0	1.0	-0.4	-0.4	-3.3	37.9	242.2	1.500	1.595	0.000
LC06	1.0	1.0	-1.0	0.4	0.4	-30.9	0.6	-23.3	1.307	1.595	0.000
LC07	1.0	1.0	-1.0	0.4	-0.4	-5.3	-8.6	-7.3	1.307	1.595	0.000
LC08	1.0	1.0	-1.0	-0.4	0.4	-23.6	1.1	-20.5	1.307	1.595	0.000
LC09	1.0	1.0	-1.0	-0.4	-0.4	-14.5	-9.9	-32.5	1.307	1.595	0.000
LC10	1.0	1.0	0.4	1.0	0.4	-89.3	38.6	347.3	1.307	1.595	0.000
LC11	1.0	1.0	0.4	1.0	-0.4	-68.1	41.0	348.1	1.307	1.595	0.000
LC12	1.0	1.0	0.4	-1.0	0.4	48.0	9.4	-31.5	1.307	1.595	0.000
LC13	1.0	1.0	0.4	-1.0	-0.4	33.4	9.8	49.8	1.307	1.595	0.000
LC14	1.0	1.0	-0.4	1.0	0.4	-23.5	8.1	21.8	1.307	1.595	0.000
LC15	1.0	1.0	-0.4	1.0	-0.4	-40.5	7.7	172.3	1.307	1.595	0.000
LC16	1.0	1.0	-0.4	-1.0	0.4	9.6	-7.5	-25.0	1.307	1.595	0.000
LC17	1.0	1.0	-0.4	-1.0	-0.4	27.8	-16.3	-40.4	1.307	1.595	0.000

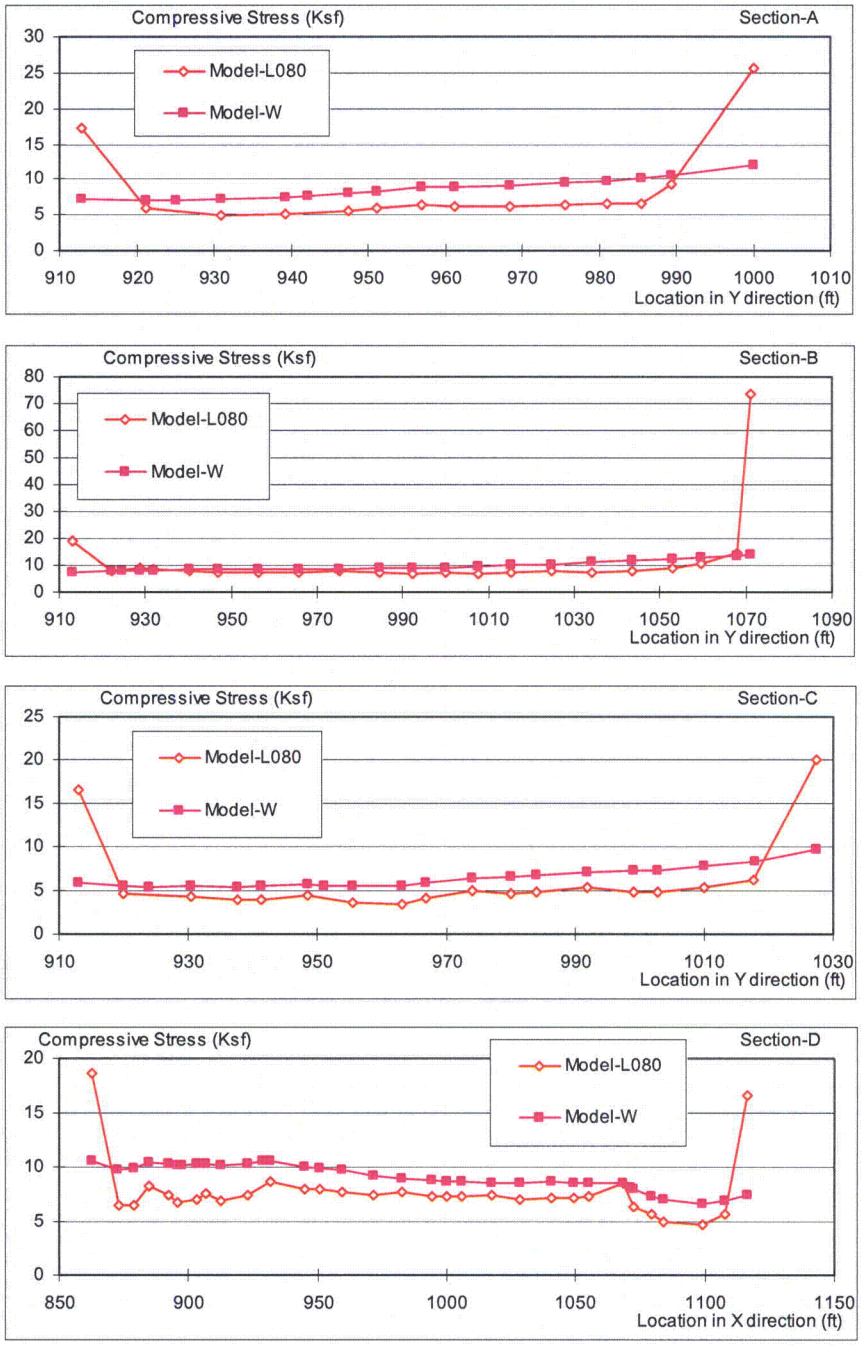

Figure RAI-TR85-SEB1-32-1
Comparison of Vertical Stress at Basemat Bottom Node – No embedment

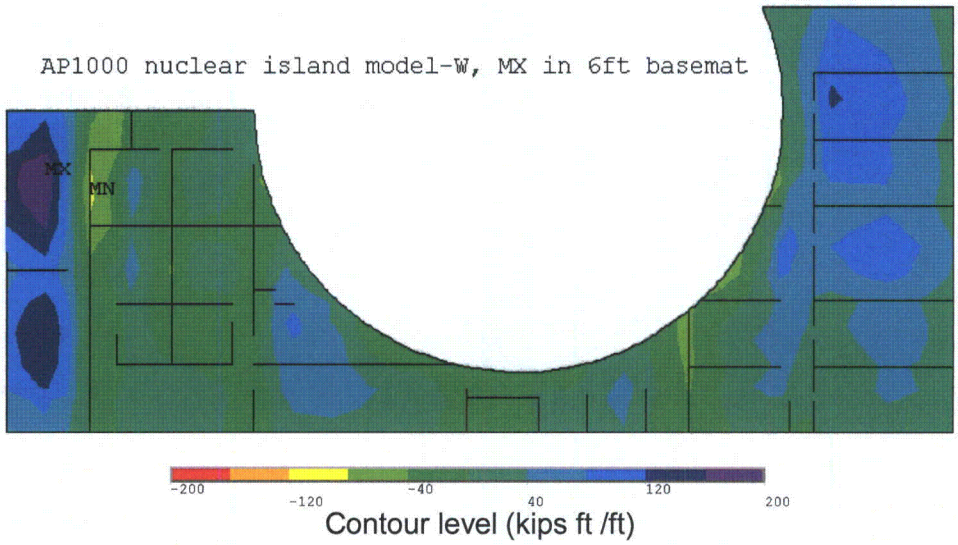

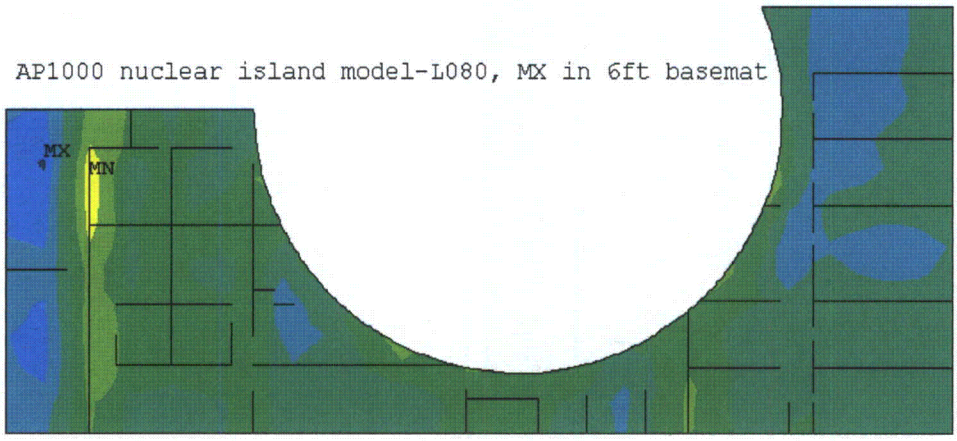

Figure RAI-TR85-SEB1-32-2 Bending Moment MX for Model-W and Model-L080

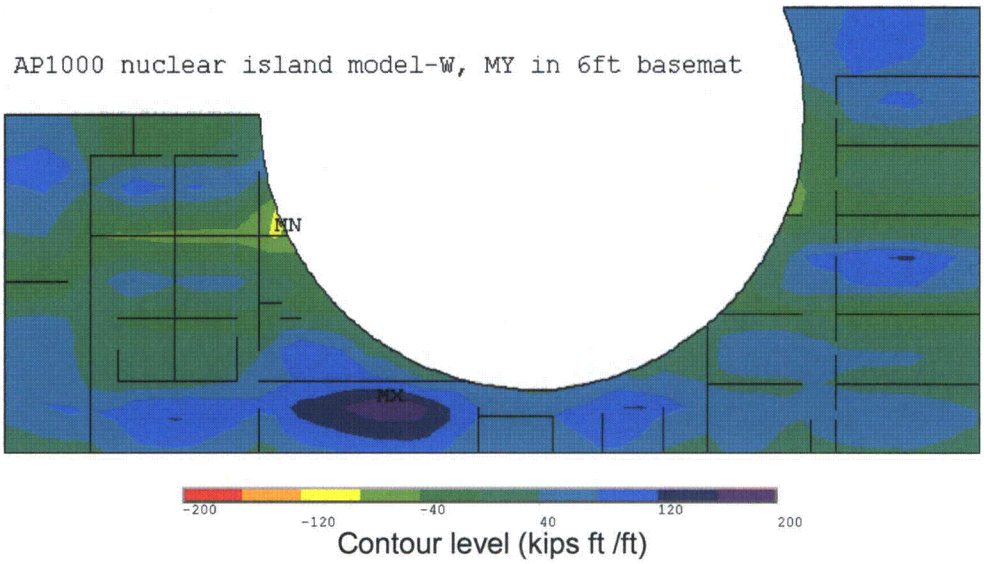

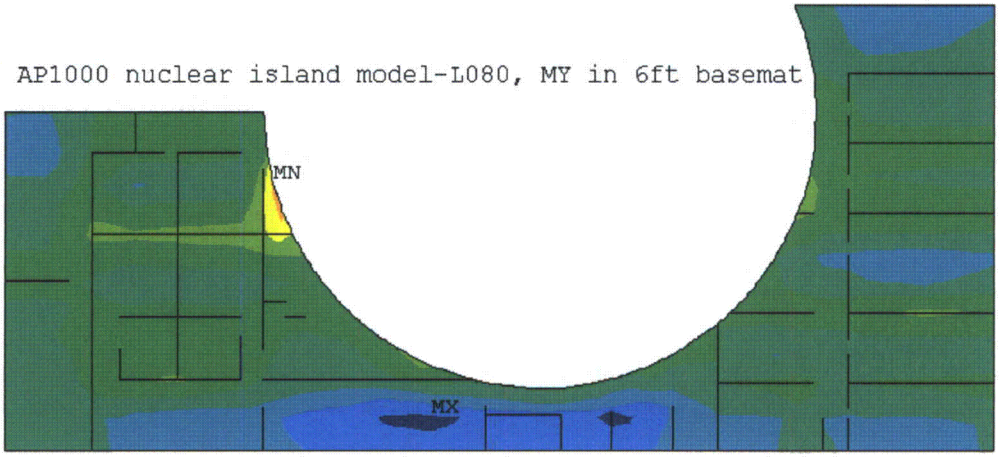

Figure RAI-TR85-SEB1-32-3 Bending Moment MY for Model-W and Model-L080

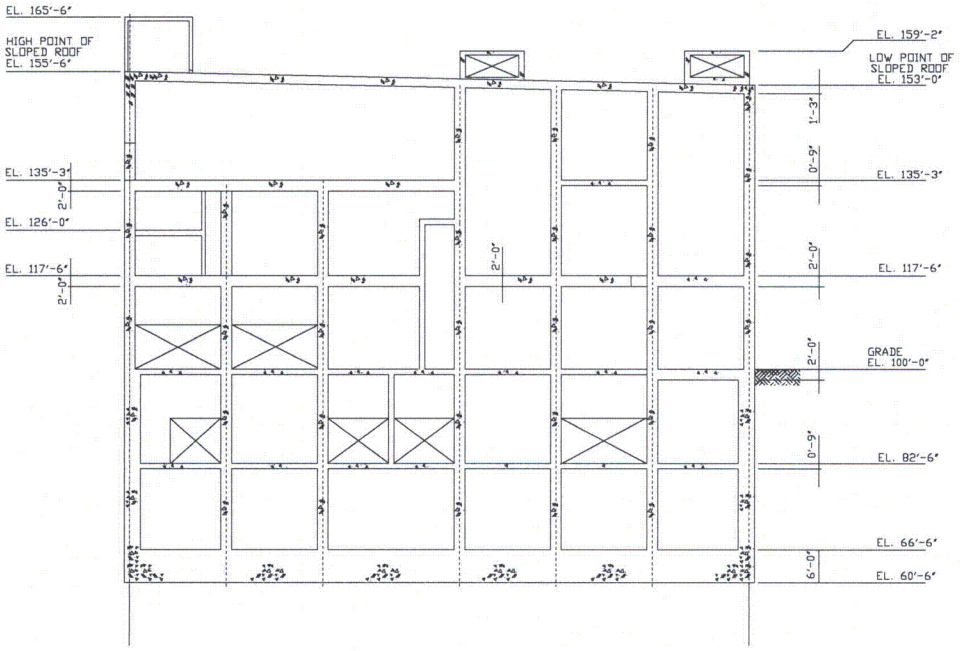

Figure RAI-TR85-SEB1-32-4

Cross section through north end of auxiliary building looking south

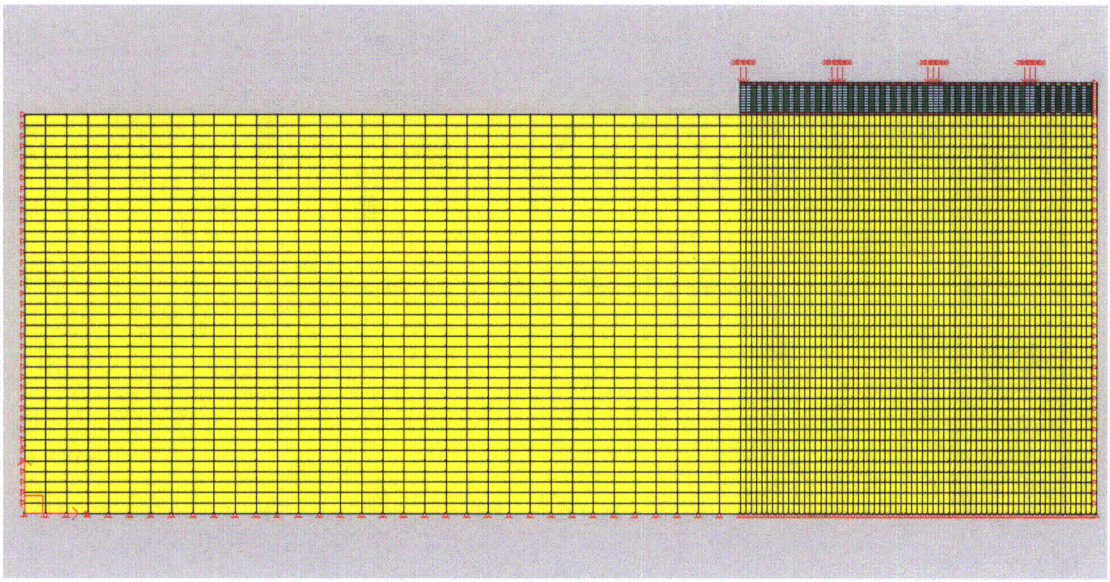

Figure RAI-TR85-SEB1-32-5

Vector2 model looking north with Soil Elements

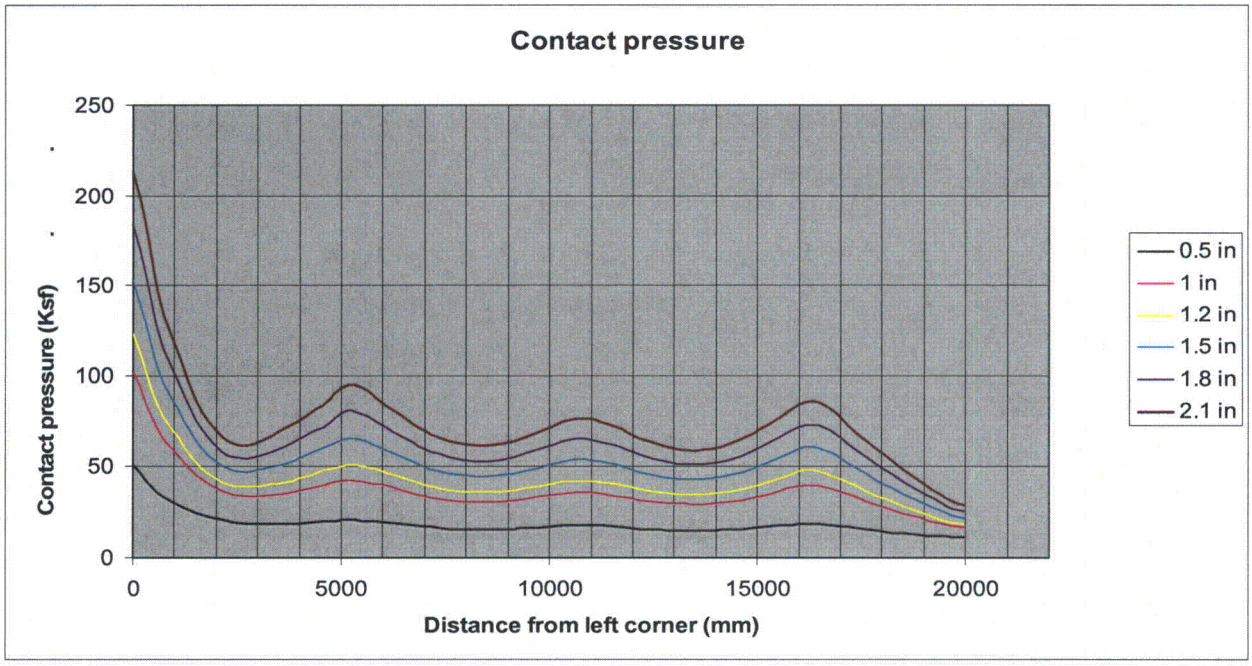

Figure RAI-TR85-SEB1-32-6
Contact Stresses along Mat for Half Space

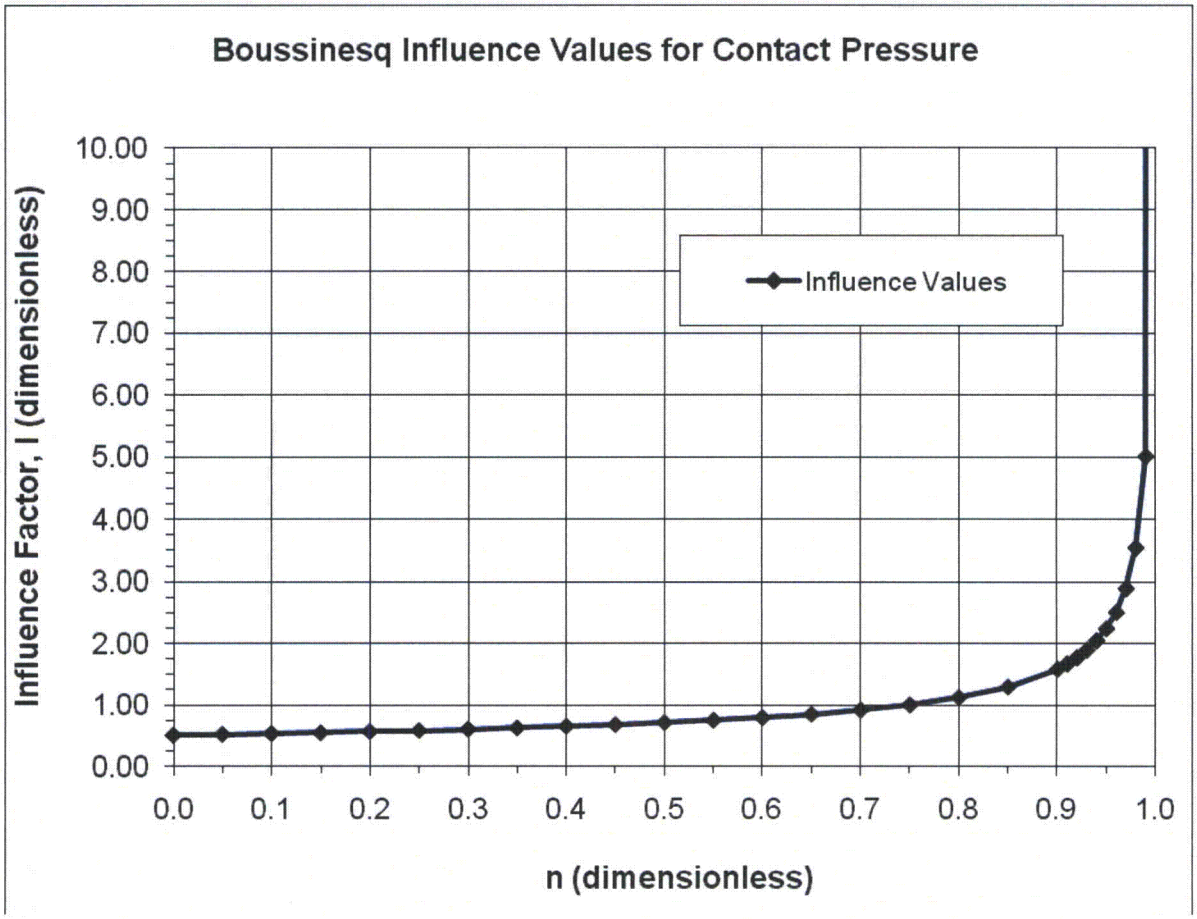

Notes:
Area (sf) = 32,480 (for NI footprint)
r (ft) = 101.68 (r for equivalent area)
If n = 0.0 is the center of the area (r = 0.0 ft)
then n = 1.0 at the perimeter (r = 101.68 ft),

Boussinesq Method (rigid circular footing)
Qo = Footing Contact Pressure
P = Foundation Load, A = Footing Area
$Qo = (P / A) \times (1 / 2x(1-n)^{0.5})$

with $I = \dfrac{1}{2\,(1-n)^{0.5}}$

Figure RAI-TR85-SEB1-32-7
Boussinesq Influence Values for Footing Contact Pressure
(rigid circular footing at ground surface, for half space)

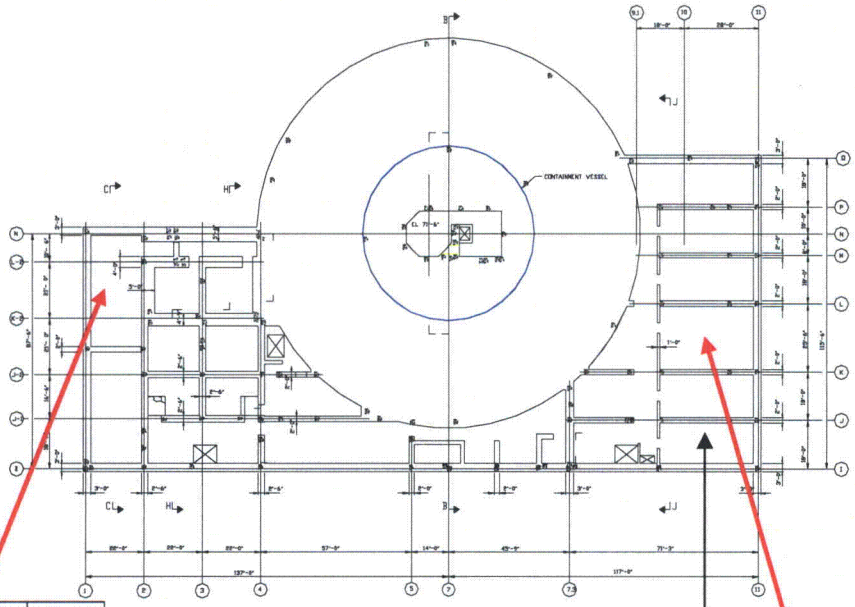

430	445	460
429	444	459
428	443	458
427	442	457
426	441	456
425	440	455
424	439	454

	715	728	742	761	780	799	818
704	714	727	741	760	779	798	817
694	703	713	726	740	759	778	797	816
693	702	712	725	739	758	777	796	815
692	701	711	724	738	757	776	795	814

Figure RAI-TR85-SEB1-32-8 Element numbers for Table RAI-TR85-SEB1-32-2

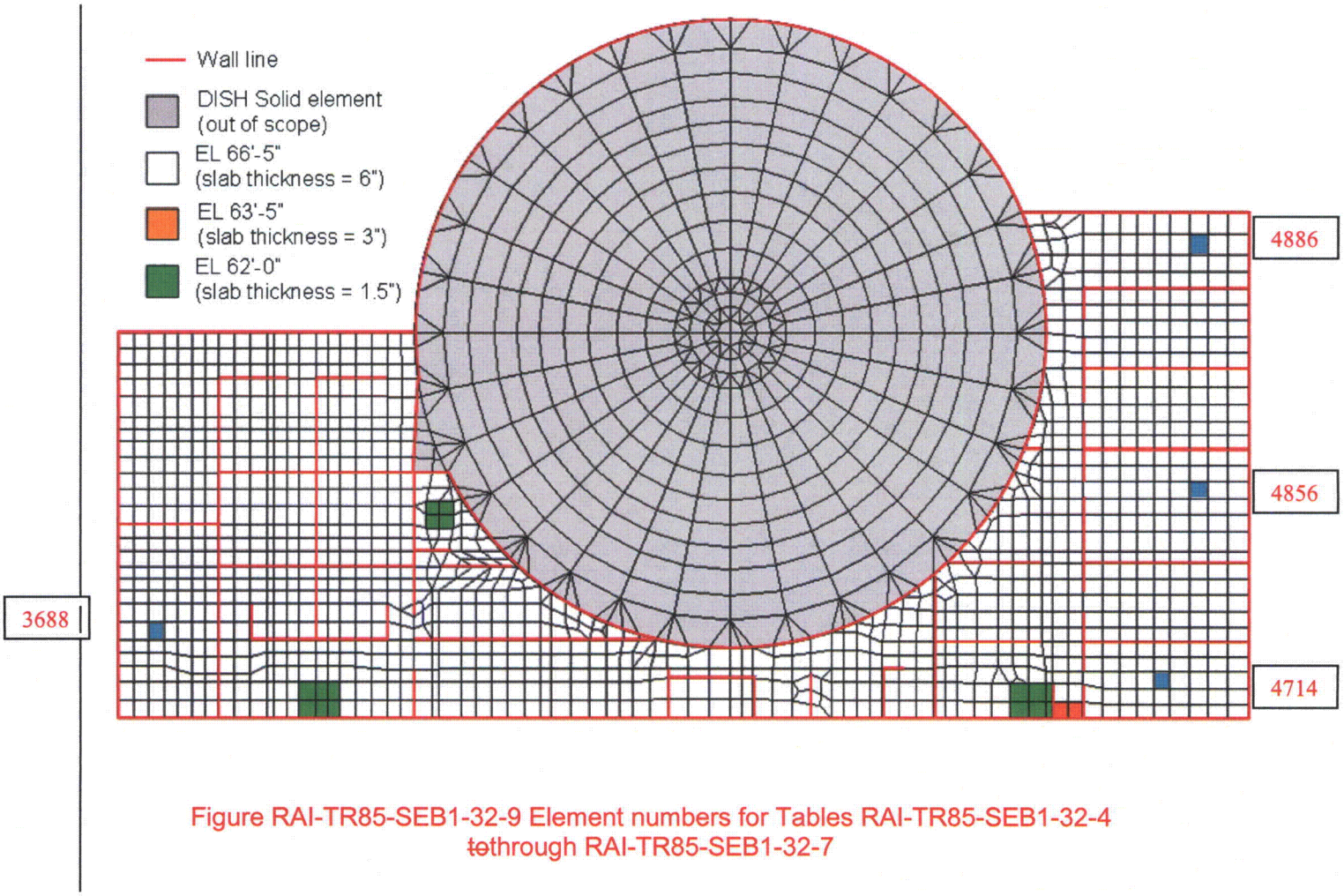

Figure RAI-TR85-SEB1-32-9 Element numbers for Tables RAI-TR85-SEB1-32-4 ~~to~~through RAI-TR85-SEB1-32-7

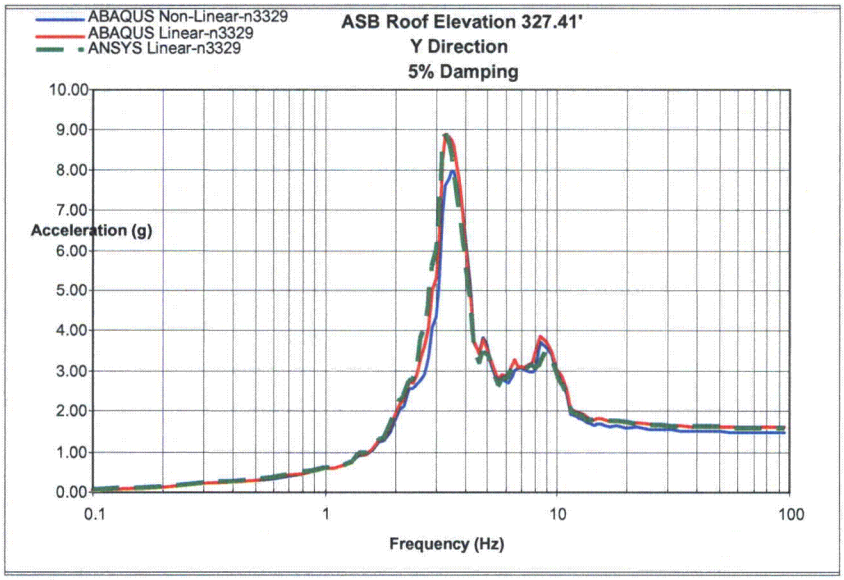

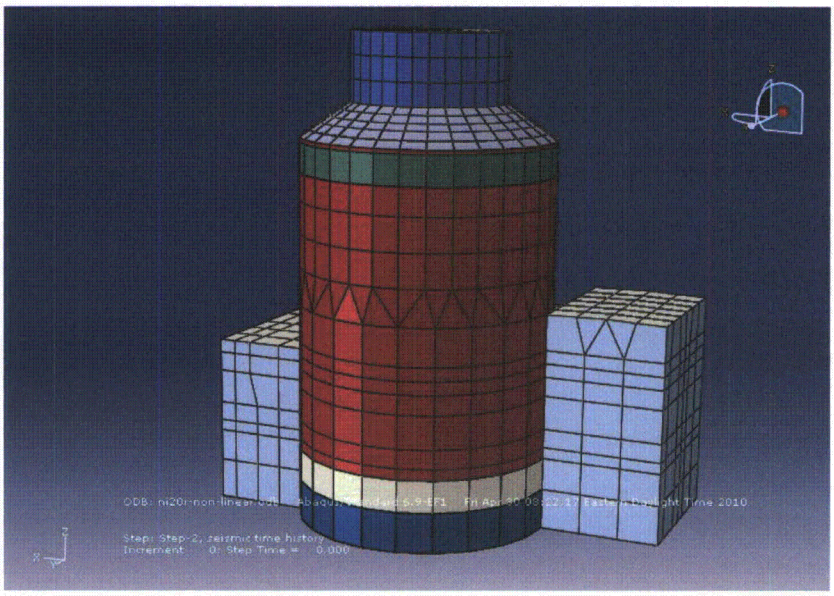

Figure RAI-TR85-SEB1-32-10 FRS Comparison at Shield Building Roof Elevation from ABAQUS Nonlinear Time History Analysis

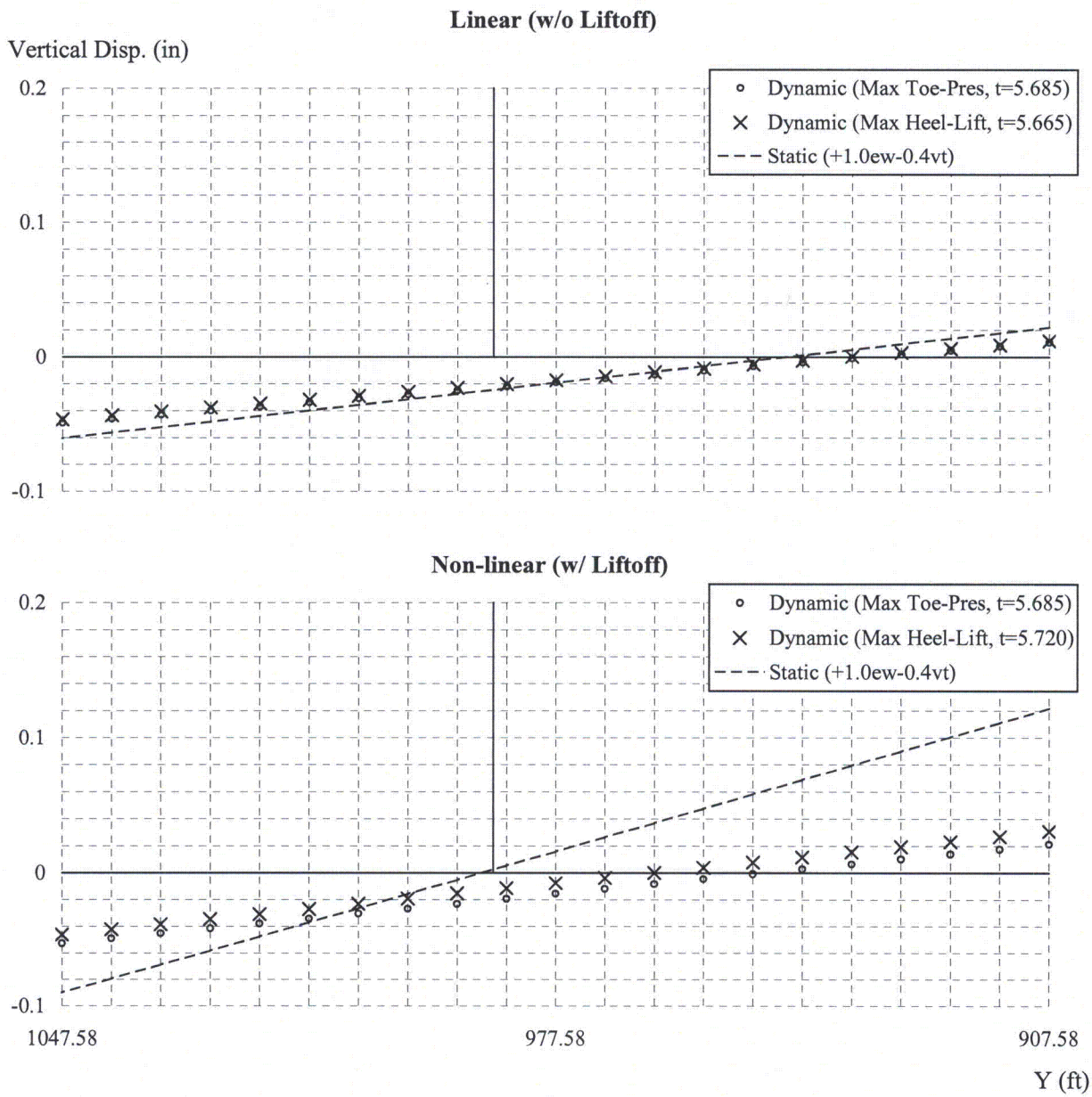

Figure RAI-TR85-SEB1-32-11 Displacement ~~c~~Comparisons ~~b~~Between ~~d~~Dynamic and ~~e~~Equivalent ~~s~~Static ~~c~~Cases

Design Control Document (DCD) Revision:
All changes to the DCD shown in this section are from previous revisions of this RAI. No additional changes have been made to the DCD in Rev 4 of this response.

The changes to the DCD shown in Rev 0 of this RAI response have been implemented in DCD Rev 17. Revise first paragraph of DCD Rev 17 subsection 2.5.4.2 as follows:

2.5.4.2 Bearing Capacity

The maximum bearing reaction determined from the 3D SASSI analyses described in Appendix 3G is less than 35,000 lb/ft^2 under all combined loads, including the safe shutdown earthquake. ~~These analyses use uniform soil springs below the basemat.~~ The maximum dynamic bearing demand of 35 ksf occurs under the west edge of the shield building and is primarily due to the response to the east-west component of the earthquake. The east edge of the nuclear island lifts off the soil. The Combined License applicant will verify that the site-specific allowable soil bearing capacities for static and dynamic loads at the site will exceed the static and dynamic bearing demand given in Table 2-1. ~~The evaluation may be limited to response in the east-west direction since the bearing demand is lower in the north-south direction.~~

PRA Revision:

None

Technical Report (TR) Revision:

Revise Tables 2.6-2 (b), 2.6-2 (c) and 2.6-4 as shown below:

Table 2.6-2 (b), revise footnote 2 as follows:

2. Equivalent static results ~~for three directions are combined by SRSS~~are shown for the response from one direction, (i.e FX and MYY due to X input, FY and MXX due to Y input, and FZ due to Z input. The increase due to combination of three directions is small.

Table 2.6-2(c)

Maximum soil bearing pressures (ksf) at corners from basemat reactions

Location	Equivalent static accelerations Linear analyses	Fixed base time history all soils
West side of shield building	~~35.9~~36.8	36.9
NW corner of auxiliary building	~~24.4~~27.1	24.8
NE corner of auxiliary building	~~25.1~~22.8	25.5
SE corner of auxiliary building	~~24.7~~21.1	25.1
SW corner of auxiliary building	~~27.0~~29.6	27.1

Table 2.6-4, revise footnotes as follows:

Note 1: See Figures 2.6-9 and 2.6-10 for plan and elevation schematic views of the reinforcement layout.

Note 2: Figures 6-1 and 6-2 in APP-1010-CCC-004, Rev.0 provide graphical presentation of the "Required" (red dash line) and "Provided" (solid black line) areas of radial reinforcement for the top face of the Dish.